

# Low temperature MBE grown GaAs for terahertz radiation applications

A. Krotkus<sup>1</sup>, K. Bertulis<sup>1</sup>, and R. Adomavičius<sup>1</sup>

<sup>1</sup>Semiconductor Physics Institute, 2600, A. Gostauto 11, Vilnius, Lithuania, phone 370 5 2616821

**Abstract:** - Attempts to optimize recombination characteristics of LTG GaAs layers for their use in terahertz (THz) radiation devices were performed. Femtosecond laser based transient reflectivity and optical pump – THz or mid-IR probe techniques were employed for the electron and, respectively, hole trapping time determination. THz range devices manufactured from LTG GaAs layers grown and annealed at different temperatures were investigated.

## I. INTRODUCTION

Low temperature molecular-beam-epitaxy grown GaAs (LTG GaAs) became lately the main material for a variety of ultrafast optoelectronic semiconductor devices because of a unique combination of its properties: high resistivity, relatively large electron mobility, enhanced breakdown field, and shorter than 1 ps carrier lifetimes [1]. Devices manufactured from LTG GaAs have successfully been used for subpicosecond electrical pulse generation [2], for broadband terahertz radiation detection [3], and as optical mixers of two laser wavelengths for CW terahertz radiation generation [4].

Despite of a large amount of work done on LTG GaAs, its properties are still far from being completely understood, thus preventing the final optimization of device structures made from this material. This is caused by several factors; two of them, which are, in our opinion, most important, would be: experimental difficulty of measuring carrier relaxation at subpicosecond time scale typical for the mentioned above materials and uncertain determination of the technological parameters critical for MBE growth at reduced substrate temperatures. These two factors cause significant scatter in the values of parameters determined by various authors and, sometimes, in very conflicting explanations of the observed phenomena.

In the present contribution we will discuss the dynamic characterisation of LTG GaAs, techniques for the determination of electron and hole trapping times in this

material, and optimisation of these parameters for the applications in THz radiation emitters and detectors. We will also describe the technology and characteristics of such devices.

## II. CARRIER TRAPPING PARAMETERS

Nonequilibrium carrier density relaxation in LTG GaAs occurs on picosecond time scale, therefore ultrafast lasers and optical techniques is the only choice for their characterisation. In LTG GaAs, carrier dynamics was documented by investigating photocurrent transients [1], pump-and-probe reflectance [5] and transmittance [6], time-resolved photoluminescence [7], and optical pump THz radiation probe experiments [8]. All these

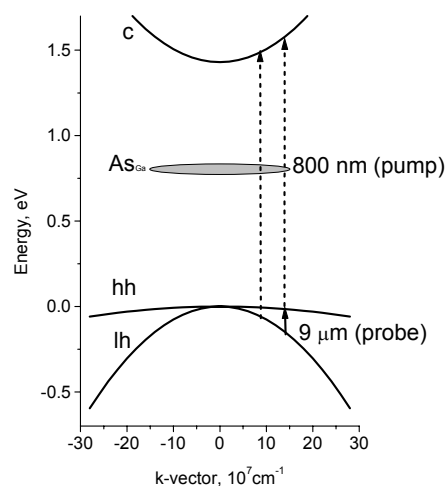


Fig. 1 Energy band structure of LTG GaAs.

experimental techniques are predominantly sensitive to the presence of the electrons in the sample; therefore, the electron dynamics in LTG GaAs is fairly good understood. In the present work, optical pump – THz probe experiment was chosen, because it provides information on both electron trapping time and their mobility values.

The information on the hole trapping processes in LTG GaAs and related materials is scarce, although for the devices manufactured from these materials and working at high repetition frequencies it is as essential as the electron trapping parameters. In [8] we proposed a technique for a direct monitoring of the hole density dynamics in the valence band of GaAs by using two-colour, pump-and-probe technique. Hole trapping time was, in this case, determined by photoexciting the carriers with near-infrared (800 nm) pulses and by probing the intervalence band transitions with 9- $\mu\text{m}$ - wavelength optical pulses. The later wavelength corresponds to the resonance transitions between the heavy and light hole

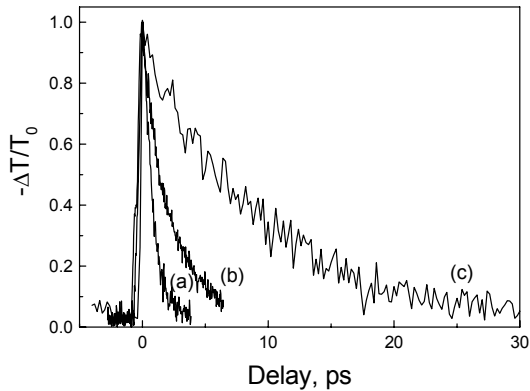


Fig. 2. Induced absorbance transients measured on as-grown LTG GaAs samples. a) Si-doped layer, b) undoped layer, c) Be-doped layer.

valence bands (Fig. 1).

The results of such measurement performed on different as-grown and annealed LTG GaAs samples are presented in Figs. 2 and 3, respectively. The decay time for pump-induced MIR transmittance, which we interpret as the hole trapping time, was close to 2 ps in as-grown, undoped layer, decreased to less than 1 ps in as-grown, Si-doped layer, and increased to  $\sim 10$  ps in as-grown, Be-doped samples. The dynamics of the hole decay was nearly independent on the photoexcitation intensity, except for Be-doped sample, where slight increase of the hole trapping time was evidenced at the largest intensities. Thermal annealing of the layers leads to significant increase of the hole trapping times (Fig.3).

LTG GaAs is highly nonstoichiometric, therefore carrier lifetimes in this material are mainly controlled by intrinsic, stoichiometry-related defects. It has been commonly assumed that ultrashort, subpicosecond electron trapping times in LTG GaAs are caused by ionized arsenic antisite defects ( $As_{Ga}^+$ ), which have large electron capture cross-section of  $\sigma_e = 10^{-13} \text{ cm}^2$  [9]. On the other hand, the density of neutral antisite

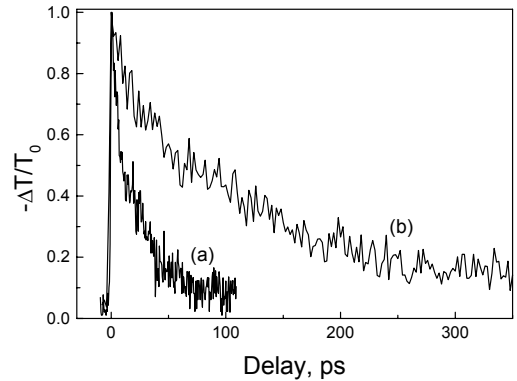


Fig. 3. Induced MIR absorbance transients measured on annealed LTG GaAs samples. a) undoped layer, b) Be-doped layer.

defects  $As_{Ga}^0$  in as-grown LTG GaAs layers is much higher than that of ionized defects, typically exceeding  $10^{20} \text{ cm}^{-3}$ . This density decreases and more As-antisites become ionized, when the layers are doped during the growth with Be; opposite effect could be expected for Si-doping. Thermal annealing of LTG GaAs layers at 600 °C and higher temperatures leads to the reduction of the overall As-antisite density by more than an order of magnitude.

All these features correlate with the observed hole trapping time dependencies on the doping or thermal treatment type. Hole trapping time is shorter for Si-doped samples and longer for Be-doped samples. It also increases after annealing of the investigated LTG GaAs layers. Moreover, the features of the observed hole dynamics at high photoexcitation intensities typical to the trap saturation are evidenced in those cases when the reduction of ionized  $As_{Ga}^0$ -density could be expected, e.g., in Be-doped or annealed samples. This suggests that capture at neutral As-antisites is the main hole trapping mechanism in LTG GaAs.

### III. THZ DEVICE TECHNOLOGY

Epitaxial LTG GaAs layers were grown on semi-insulating (100)-oriented GaAs substrates in a solid-state molecular-beam epitaxy (MBE) system. The growth temperature of the LTG layer measured by a thermocouple fixed to the substrate holder was 270 °C; a growth rate of 1.5  $\mu\text{m}/\text{h}$  was used for all growth runs. The thickness of LTG GaAs layers were 1.5  $\mu\text{m}$ . During the growth of two layers,  $As_4/Ga$  beam-equivalent pressure ratio was kept equal to 10; one of those layers was annealed after the growth in the growth chamber for 20 min at the temperature of 600 °C (layer A), the second – at the temperature of 450 °C (layer B). The third layer

(layer C) was grown at slightly lower substrate temperature of 250 °C and was annealed at the temperature of 600 °C. Electron trapping time in layer A determined by optical pump – THz probe technique was  $\sim 1.7$  ps; the hole trapping time measured in [8] by optical pump – MIR probe method was 20 ps. Electron trapping time of the layer C was 0.6 ps. Electron trapping time of a similar magnitude was also evidenced for the layer B. Results of optical pump – THz probe measurements for two of the investigated LTG GaAs layers are presented on Fig. 4. In both cases photoexcited carrier density was

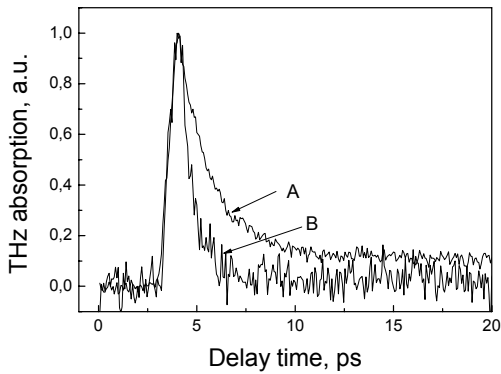


Fig. 4 Electron density dynamics in two LTG GaAs layers monitored by the optical pump – THz probe measurement.

$4 \cdot 10^{16} \text{ cm}^{-3}$ ; the traces shown in the Figure are normalized to their maxima.

5-mm-long Hertzian dipole type antennae were patterned from an evaporated 200-nm-thick Au film with a 5-nm-thick Ti adhesion layer. The dipole consisted of a coplanar strip-line section with a photoconductive gap in the centre of the strip-line. The width of the strip-line conductors was 20  $\mu\text{m}$  and the distance between the conductors was 80  $\mu\text{m}$ . Dipoles with 5- $\mu\text{m}$ -wide photoconductive gaps were used as THz radiation detectors; THz radiation was generated by devices with various gap widths. Moreover, besides of these MSM devices, THz emitters were also manufactured from an epitaxial structure with a heavily p-type doped GaAs layer on top of LTG GaAs.

Standard THz radiation system based on devices made from LTG GaAs was activated by mode-locked Ti-sapphire (Mira, Coherent) laser pulses (duration of 120 fs, repetition rate of 76 MHz, central wavelength of 815 nm). Average laser power of 10 mW was used for operating photoconductive detectors from LTG GaAs for THz pulse sampling; the average power of the beam exciting THz emitters was changed from 10 to 200 mW.

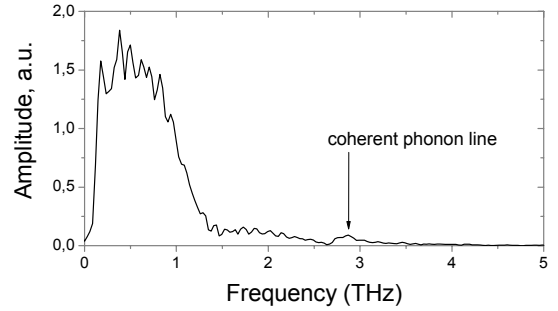


Fig. 6 THz emission from crystalline Te surface demonstrating broad band property of LTG GaAs detector.

#### IV. THz COMPONENTS FROM LTG GaAs

Let us first consider the characteristics of THz detectors manufactured from different LTG GaAs layers. In the present study, separate characterization of the detectors was done by using the radiation from femtosecond laser

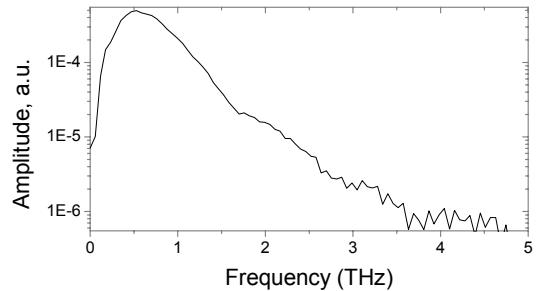


Fig. 5 Spectral response of the detector made from LTG GaAs layer C.

pulse excited surface of InAs crystal as a THz radiation source. In the case of photoexcited InAs surfaces, the main effect causing THz emission is electrical-field-induced optical rectification, therefore, the bandwidth of this emission will be determined by the optical pulse duration. Figs. 5 and shows THz radiation spectra measured by the detector manufactured from the layer C. This spectrum was obtained by photoconductive sampling of the transients generated by InAs emitter and by performing fast-Fourier-transformation on those transients. It could be seen from Figure 5 that frequency corresponding to the maximum of the spectral

dependence for detector made from the layer C ( $f \sim 600$  GHz) correlates with the electron trapping time in that layer ( $f \sim 0.35/\tau_n$ ). This is true also for detectors manufactured from the layer A, for which frequency of the maximum signal is lower ( $f \sim 400$  GHz). Although at frequencies above this maximum the emitted THz power is decreasing quite fast with the frequency, the signal is larger than the noise even at the frequencies close to 3 THz. This is demonstrated by the measurement of coherent phonon line at 2.9 THz [9], observed from the laser illuminated surface of tellurium crystal (Fig. 5). The frequency characteristics of the detectors manufactured from the layer B were similar to those made from the layer C, but their sensitivity was more than 10 times worse. Most probably, the reduction of the sensitivity is caused by lower electron mobility in a LTG GaAs layer in the case when it was insufficiently annealed.

One of the most important parameters of THz emitters is their electrical breakdown field. Larger breakdown fields lead to larger power radiated by the device. Fig. 7 shows the dependences of the radiated THz power on the dipole antenna bias voltage for two different types of the contact structure with photoconductive gap lengths of 5  $\mu\text{m}$ . Both dipoles were made on the LTG GaAs layer B.

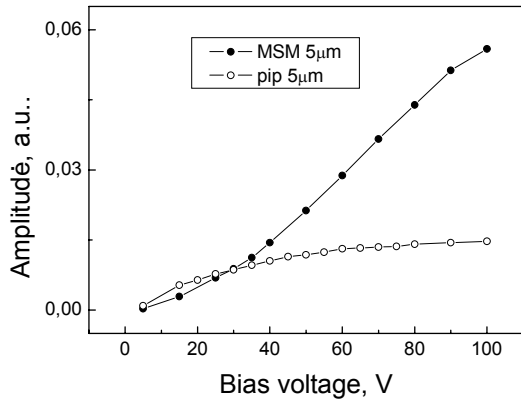


Fig. 7 Dependence of the THz field magnitude on the photoswitch bias voltage for two types of the contact structure. LTG GaAs layer B was used for manufacture of both switches; average laser power used for the photoexcitation was 40 mW.

As it can be seen from the Figure, both dependences are strikingly different. The amplitude of THz signal emitted by the p-i-p structure saturates rather fast with the increasing bias voltage. On the other hand, THz emission from the structure with MSM type contacts continues to increase up to the breakdown of the photoconductive gap. Breakdown fields correspond to  $\sim 250$  kV/cm, which is close to the onset of the impact ionisation in GaAs. This difference could be explained by the photoconductive

gain effect that might be possible in MSM structures, but not in p-i-p structures with the contacts blocking the electron flow. In the later case, to the photocurrent transient producing THz radiation contribute only the photoexcited electrons and holes. Drift velocities of both those types of current carriers are saturated in GaAs at fields higher than  $\sim 30$  kV/cm, which explains the saturation of the emitted THz power. This assumption is confirmed by the experiments performed on p-i-p structures with a 80- $\mu\text{m}$  long photoconductive gap. For these structures THz signal magnitudes also saturate at fields of 30 kV/cm. One has to point out that THz radiation from the dipoles with MSM contact structure and 80- $\mu\text{m}$  long photoconductive gap was quite powerful and was easily detected by a pyroelectric detector working at room temperature.

## V. CONCLUSIONS

Electron and hole trapping times in LTG GaAs layers were characterised by original two-color, pump-and-probe techniques. Probe wavelength was equal to 9  $\mu\text{m}$  for measuring the hole dynamics and in THz frequency range for monitoring the photoexcited electron decay. Various device structures for THz radiation detection and emission were manufactured and characterised; these results are discussed in terms of LTG GaAs material parameters.

This work was, in part, supported by NATO "Science for Peace" project SfP-977978.

## REFERENCES

- [1] F.W. Smith, H.Q. Le, V. Diaduk, M.A. Hollis, A.R. Calawa, S. Gupta, M. Frankel, D.R. Dykaar, G.A. Mourou, and T.Y. Hsiang, *Appl. Phys. Lett.* v. 54, p. 890, 1989.
- [2] P. Kordos, A. Forster, M. Marso, and F. Ruders, *Electron. Lett.* v.34, p.119, 1998.
- [3] S. Kono, M. Tani, and K. Sakai, *Appl. Phys. Lett.* v.79, p.119, 2001.
- [4] K.A. McIntosh, E.R. Brown, K.B. Nichols, O.B. McMahon, W.F. DiNatale, and T.M. Lyszczarz, *Appl. Phys. Lett.* v.67, p.3844, 1994.
- [5] J-F. Roux, J-L. Coutaz, and A. Krotkus, *Appl. Phys. Lett.* v.74, p.2462, 1999.
- [6] U. Siegner, R. Fluck, G. Zhang, and U. Keller, *Appl. Phys. Lett.* v.69, p.2566, 1996.
- [7] A. Krotkus, R. Viselga, K. Bertulis, V. Jasutis, S. Marcinkevicius, and U. Olin, *Appl. Phys. Lett.* v.66, p.1939, 1995.
- [8] S.S. Prabhu, S.E. Ralph, M.R. Melloch, and E.S. Harmon, *Appl. Phys. Lett.* v.70, p.2419, 1997.
- [9] R. Adomavicius, A. Krotkus, K. Bertulis, V. Sirutkaitis, R. Butkus, and A. Piskarskas, *Appl. Phys. Lett.* **83**, 5304, 2003.